ELSEVIER

European Journal of Cancer 41 (2005) 1474–1486

European Journal of Cancer

www.ejconline.com

Involvement of both intrinsic and extrinsic pathways in IFN-γ-induced apoptosis that are enhanced with cisplatin

Caroline Barton [a], Derek Davies [b], Fran Balkwill [a,*], Frances Burke [a]

[a] *Cancer Research UK Translational Oncology Laboratory, Barts and the London, Queen Mary's School of Medicine and Dentistry, Charterhouse Square, London EC1M 6BQ, UK*

[b] *Cancer Research UK FACS Laboratory, The London Research Institute Cancer Research UK, 44 Lincoln's Inn Fields, London WC2A 3PX, UK*

Received 30 March 2005; accepted 30 March 2005
Available online 9 June 2005

Abstract

IFN-γ has direct anti-proliferative effects on ovarian cancer cell lines and tumour cells isolated from ovarian cancer ascites. The aim of this study was to further elucidate the mechanisms involved. An IFN-γ-mediated cell cycle blockade was detectable in synchronised cell populations. Apoptosis, which was caspase dependent, was also induced. When caspase activity was blocked, the anti-proliferative effect of IFN-γ was only partially reduced indicating independent roles for both growth inhibition and apoptosis in its actions. We have demonstrated involvement of the intrinsic apoptotic pathway; IFN-γ treatment resulted in mitochondrial membrane depolarisation, cytochrome *c* release into the cytosol and activation of caspase 9. Cytochrome *c* release was blocked by the presence of a general caspase inhibitor, suggesting a role for caspases upstream of the mitochondria. One candidate is caspase 8, which was also activated in cells treated with IFN-γ. Levels of Bid, a pro-apoptotic molecule that can mediate mitochondrial membrane permeabilisation when cleaved by caspase 8, were also decreased and indicated a potential link between these two pathways in IFN-γ-induced apoptosis. Furthermore, together with cisplatin, IFN-γ exerted a more powerful anti-proliferative effect.

Keywords: IFN-γ; Apoptosis; Caspase; Cisplatin

1. Introduction

Extensive experiments in a range of animal cancer models suggest that endogenous IFN-γ is involved in immune surveillance of tumours via a combination of lymphocyte mediated responses, direct actions on tumour cells and inhibition of tumour angiogenesis (reviewed in [1]). Studies looking at the direct effects of human IFN-γ on tumour cells revealed that this cytokine inhibited the growth of human ovarian tumour xenografts growing in nude mice [2]. Both DNA synthesis was inhibited and apoptosis induced [3]. Human IFN-γ can also directly inhibit the growth of human ovarian cancer cell lines and primary ovarian epithelial cancer cells derived from patients ascites *in vitro*. Again this was associated with the induction of apoptosis [4,5]. These effects required 2–3 days of exposure to IFN-γ for an irreversible effect on cell survival. A pilot study, conducted to see whether exogenous IFN-γ-induced cell death *in vivo*, showed that 2/6 patients had a 90% reduction in the number of tumour cells in ascites after treatment; some of this response could be attributed to apoptosis [5]. Clinical benefit as assessed by intervals in paracentesis was observed in these two patients.

In addition to its ability to induce apoptosis in ovarian cancer cells, IFN-γ can also initiate apoptosis in other cell types and/or sensitise them to subsequent death signals delivered by mediators such as TNF

* Corresponding author. Tel.: +44 20 7882 6106; fax: +44 20 7882 6110.
E-mail address: frances.balkwill@cancer.org.uk (F. Balkwill).

0959-8049/$ - see front matter © 2005 Elsevier Ltd. All rights reserved.
doi:10.1016/j.ejca.2005.03.022

superfamily members. This involves the induction of a number of apoptotic-related genes involved in both the extrinsic and intrinsic apoptosis pathways. IFN-γ-induced apoptosis has been associated with caspase upregulation and activation. For example, in human erythroid colony-forming cells (ECFC), IFN-γ upregulates and activates caspases 2, -6, -8 and -9 [6] and in colorectal adenocarcinoma cell lines IFN-γ activates caspase 8 and caspase 3 thus triggering apoptosis [7]. In other cell types e.g. breast and colon carcinoma cells, and lung epithelial cells, IFN-γ enhances caspase 8 expression which sensitises cells to apoptosis by CD95L/TRAIL [8–11]. IFN-γ also regulates members of the Bcl-2 family, decreasing expression of anti-apoptotic molecules such as Bcl-2 and Bcl-X_L and increasing expression of pro-apoptotic molecules, e.g. Bax/Bak [12].

IFN-γ can also induce growth arrest in a number of cell types. The progression of cells through all phases of the cell cycle can be slowed by IFN-γ [13], although in some cells there are more pronounced effects on G_1/G_0 [14]. Differences in the point of cell cycle arrest indicate that diverse growth inhibitory mechanisms are employed by IFN-γ.

Clinically, ovarian cancer remains a difficult disease to treat since most patients present with advanced disease. A regime of platinum-taxol chemotherapy following cytoreductive surgery is common, but patients often relapse. A number of clinical studies show that IFN-γ has some activity against advanced ovarian cancer. In a phase II trial, 108 patients with residual disease documented at second look laparotomy after first line cisplatin-based chemotherapy, were treated with intraperitoneal, i.p., IFN-γ twice a week for three-four months [15]. Of 98 assessable patients, 23 achieved complete and eight partial response. In a randomised phase III study, 148 women treated with cisplatin and cyclophosphamide as first line chemotherapy for ovarian cancer were randomly allocated to receive additional IFN-γ three times weekly on alternate weeks [16]. IFN-γ administration was associated with a significant increase in progression free survival but an observed increase in overall survival was not statistically significant. A large global randomised phase III trial, GRACES (Gamma Interferon and Chemotherapy Efficacy Study), is currently in progress to assess the activity of IFN-γ in combination with platinum and taxol.

In this study we sought to investigate further the mechanisms behind the direct anti-proliferative activity of IFN-γ in ovarian cancer cell lines. We also looked at the effects of IFN-γ used in combination with cisplatin, an agent commonly used in ovarian cancer. Further analysis of the molecular events involved in IFN-γ-induced apoptosis may aid identification of cancer patients that are most likely to respond to combination therapy with this cytokine.

2. Materials and methods

2.1. Cell lines

PEO1 was derived from ascites in a patient with poorly differentiated adenocarcinoma and were obtained from Dr. S. Langdon, Cancer Research UK Edinburgh Medical Oncology Unit, UK. OVCAR-3 originated from ascites in a patient with poorly differentiated papillary adenocarcinoma (purchased from the American Type Culture Collection [ATCC]).

2.2. Tissue culture

All cell lines were grown in a humidified atmosphere at 37 °C (10% CO_2) under pyrogen-free conditions. Cells were grown in RPMI 1640 (Invitrogen, UK) supplemented with 10% FBS (Autogen Bioclear, UK), 5 μg/ml insulin, 2 mM L-glutamine, 100 U/ml penicillin and 100 μg/ml of streptomycin (Sigma, UK). All cells were free from and routinely checked for mycoplasma.

2.3. Reagents

Recombinant human IFN-γ was provided by Roussel UCLAF as a lyophilised preparation (20 MU/vial) and was more than 95% pure. Endotoxin levels were less than 0.24 UE/vial and the specific activity was 3×10^7 units/mg protein. Cisplatin [*cis*-diamminedichloroplatinum (II)] (Sigma, UK) was diluted in dimethyl sulphoxide (DMSO) (Sigma, UK) at 25 mg/ml immediately before use. The following reagents were reconstituted in DMSO and stored at −20 °C: Staurosporine (STS) (Sigma, UK) was at 1 mM; z-VAD-FMK and z-FA-FMK (ICN Biomedicals Inc, UK) at 20 mM; Nocodazole (Sigma, UK) at 5 mg/ml. Hydroxyurea (Sigma, UK) was reconstituted in sterile H_2O at 1 M immediately before use.

2.4. Proliferation assays

Cell lines were seeded at 1×10^5 cells/well of a 6 well plate and counted using a Vi-Cell$_{XR}$ counter (Beckman Coulter, UK).

2.5. Protein extraction

Preparation of total cell lysates. Cells were cultured in 6 well plates and were seeded at concentrations that would ensure the cells were just confluent at the time of harvest. Non-adherent cells were collected from the supernatant by centrifugation and combined with adherent cells. Cells were lysed using ice-cold lysis buffer (62.5 mM Tris–HCl, pH 7.4, 1% SDS). Lysates were passed through a 25 g needle and protein estimation

was performed using a standard BCA assay (Sigma, UK) according to the manufacturer's instructions.

Preparation of mitochondrial and cytosolic lysates. Cells were cultured in 175 cm^2 flasks until just confluent at the time of harvest. Lysates were prepared using the Clontech ApoAlert® Cell fractionation Kit (BD Biosciences, UK), according to manufacturer's instructions. Adherent and non-adherent cells were pooled. Cells were homogenised in a 1 ml Dounce Tissue grinder (Zinseer, UK) on ice with 50 passes of the grinder. Protein estimation was performed using the Bio-Rad protein Assay System (Bio-Rad Laboratories, Munich, Germany) according to the manufacturer's instructions.

Lysates were combined with 5× loading buffer (312.5 mM Tris–HCl, pH 6.8, 10% SDS, 20% glycerol, 10% β-mercaptoethanol, 1% w/v bromophenol blue, [all from Sigma, UK]). The samples were boiled at 100 °C for 5 min, then cooled on ice before being stored at −80 °C.

2.6. SDS-PAGE

Electrophoresis was performed using standard conditions. 20 μg of total protein or 5 μg cytosolic/mitochondrial lysates were loaded onto the gel. The percentage acrylamide gel used depended on the molecular weight of the protein and ranged from 10% to 15%. Protein lysates were run at 120 V for 2 h on an AE-6400 Dual Mini slab kit gel electrophoresis system (Atto Bioscience, MD, USA) using 1 × running buffer (Tris 25 mM, Glycine 192 mM, SDS 0.1%). Blue pre-stained protein standard markers (Invitrogen, UK) were used to determine product size.

2.7. Western blotting

Protein was transferred to nitrocellulose (Hybond-ECL, Amersham International, UK), pre-equilibrated in transfer buffer (Tris 25 mM, Glycine 192 mM, methanol 20%) using a Trans-Blot electrophoretic transfer cell (Bio-Rad, UK) for 2 h at 50 V. Blots were blocked and then incubated in primary antibody (diluted in PBS-0.1% Tween 20, with either 5% BSA or 5% non-fat dry milk, according to manufacturer's instructions) overnight at 4 °C. Blots were exposed to the secondary antibody (diluted in PBS-0.1% Tween 20 with 3% non-fat milk powder) at room temperature with agitation for an hour. The Amersham ECL system was used for detection and membranes were exposed to blue-light sensitive autoradiography film (Hyperfilm ECL). Densitometry was performed using NIH Image 1.61.

2.8. Antibodies

All antibodies were purchased from NEB (UK), unless otherwise stated. Cleaved PARP, Bid, caspase 8 (BDPharmingen, Belgium) and caspase 9 antibodies were used at a dilution of 1:1000. Cytochrome *c* antibody (BDPharmingen, Belgium) was used at a dilution of 1:500 and COX-4 antibody (Cambridge Bioscience, UK) was used at a dilution of 1:2000. β actin (Sigma, UK) was used at a dilution of 1:5000.

2.9. Fluorescence-activated cell-sorting analysis (FACS) of caspase activity

Cells were grown in 6 well plates and were seeded at concentrations that would ensure that the cells were just confluent at the time of harvest. APO LOGIX FAM caspase detection kits (ApoLogix) were used to detect active caspase 8 (FAM-LETD-FMK) and caspase 9 (FAM-LEHD-FMK) *in situ*, according to manufacturer's instructions. Adherent and non-adherent cells were combined and TO-PRO-3 was added to discriminate dead cells. Cells were analysed on a FACSCalibur flow cytometer using CellQuest Software (Becton Dickinson). Fluorescence from FAM was measured in the FL1 channel (530/30 nm bandpass filter). Fluorescence from red-laser (633 nm) excitation of TO-PRO-3 was measured in the FL4 channel (661/16 nm bandpass filter), 20 000 events were collected/sample.

2.10. FACS analysis of reduction in mitochondrial membrane potential

Cells were grown in 6 well plates and were seeded at concentrations that would ensure that the cells were just confluent at the time of harvest. Adherent and non-adherent cells were harvested and combined. CMXRos (Cambridge Bioscience, UK) was added to a final concentration of 50 nM and TO-PRO-3 was added to discriminate dead cells. Cells were analysed on a FACSCalibur flow cytometer using CellQuest Software (Becton Dickinson, UK). CMXRos fluorescence was measured in the FL3 channel (670 nm longpass filter) and fluorescence from red-laser (633 nm) excitation of TO-PRO-3 was measured in the FL4 channel (661/16 nm bandpass filter). 20 000 events were collected/sample.

In addition, PEO1 cells treated with IFN-γ (5000 U/ml) for 72 h were stained with CMXRos, as outlined, and sorted into live and apoptotic populations using a FACS vantage. DAPI was used as the dead cell discriminator. Cells were fixed in 1% PFA at a concentration of approximately 5×10^5 cells/ml which was used to make cytospins. 100 μl of the cell suspension was spun onto an electrostatically charged slide ('Superfrost', BDH Laboratories, UK) at 500 rpm for 5 min using a cytocentrifuge (Shandon Cytospin3). Slides were fixed in 4% PFA for 5 min and rinsed with PBS. 5 μg/ml Hoechst 33342 (Sigma, UK) was used to stain chromatin,

visualised under a 350 nm excitation filter on a Nikon Labophot 2 microscope.

2.11. Cell cycle analysis

Cells were grown in 6 well plates and were seeded at concentrations that would ensure that the cells were just confluent at the time of harvest. BrdU was added to supernatant to final concentration of 10 μM for 30 min. Adherent cells were harvested, washed, collected by centrifugation, resuspended in PBS and drawn through a 19 g needle. Cells were fixed in ice-cold 70% ethanol, left for >30 min at 4 °C and then collected by centrifugation. Cells were prepared for staining, and stained with anti-FITC-conjugated BrdU antibody (Becton Dickinson, UK), according to manufacturer's instructions. Propidium iodide (PI) was then added. FITC emission from BrdU was measured in the FL1 channel (530/30 nm bandpass filter) and PI fluorescence was measured in the FL3 channel (670 nm longpass filter) after cell doublets were excluded by pulse processing. 20 000 events were collected/sample. G_1, S and G_2 cells were gated out as appropriate.

2.12. Statistical analysis

Students unpaired *t*-test or ANOVA were used to evaluate results from cell proliferation studies, BrdU staining, western immunoblot quantification, caspase APOLOGIX FACS and CMXRos analysis. A probability of <0.05 was considered significant. Where applicable, data are presented as the mean ± SE, unless otherwise stated.

3. Results

In two previous papers we have provided evidence that IFN-γ, at doses ranging from 10 to 5000 U/ml, has a time and dose-dependent anti-proliferative effect on the majority of ovarian cancer cell lines and freshly isolated primary tumour cells from the ascites of ovarian cancer patients *in vitro* [4,5]. Here we have attempted to determine the relative contribution of cell growth arrest and apoptosis in this action. We used two cell lines that are sensitive to the anti-proliferative effects of IFN-γ (PEO1 and OVCAR-3), which we have previously demonstrated to be representative from a larger panel of ovarian cancer cells [4,5].

3.1. IFN-γ induces a cell cycle blockade

We investigated growth arrest. Cells were treated with nocodazole to synchronise them at the G_2–M boundary or with hydroxyurea to synchronise them at the G_1–S boundary. Following synchronisation, cells were treated with media ± IFN-γ (5000 U/ml). The percentage of cells synthesising DNA was significantly decreased in IFN-γ treated populations at all time points after 48 h (Fig. 1(a)). For example, at 72 h, the percentage of IFN-γ treated cells in S phase was 33.2% compared to 43.2% of untreated cells ($P = 0.0014$, $n = 6$). Graphical representations of mean values at 72 h are shown in Fig. 1(b). Similar reductions could be seen in the percentage of S phase IFN-γ treated PEO1 and OVCAR-3 cells synchronised with hydroxyurea. For example, after 72 h of IFN-γ treatment, 27.3% of PEO1 cells were synthesising DNA compared with 39.5% of the untreated population ($P = 0.0097$) (Fig. 1(c)). Similarly, 44.9% of OVCAR-3 cells were synthesising DNA compared with 51.6% of the untreated population ($P = 0.0039$) as demonstrated in Fig. 1(d). Thus, IFN-γ-induced growth arrest in ovarian cancer cells is sensitive to its anti-proliferative effects.

3.2. IFN-γ induces PARP cleavage in ovarian cancer cell lines

We have previously demonstrated [4] that the anti-proliferative effects of IFN-γ could be partially attributed to apoptosis, as assessed by the TUNEL assay and electron microscopy. PARP is involved in DNA repair, and is one of the first proteins to be cleaved by the executioner caspases [17,18]. In this study we looked to see if cleaved PARP could be detected in PEO1 and OVCAR-3 cells following IFN-γ treatment. This molecule has previously been shown to be a sensitive marker of apoptosis and was used successfully in a pilot study to assess apoptosis induced by IFN-γ in the ascites drawn from IFN-γ treated patients [5].

The 89 kDa fragment of PARP was detected after 48 h exposure to IFN-γ in both PEO1 and OVCAR-3 cells, reaching maximal levels at 96 h (Fig. 2(a) and (b)). IFN-γ-induced PARP cleavage in PEO1 cells was unaffected by prior hydroxyurea synchronisation; cleaved PARP was also maximal at 72–96 h after IFN-treatment in hydroxyurea-synchronised cells (Fig. 2(c)). The presence of cleaved PARP following IFN-γ treatment suggested a role for the caspase family in IFN-γ-induced apoptosis.

3.3. IFN-γ-induced PARP cleavage is caspase dependent in PEO1 cells

To assess whether caspase-mediated apoptosis contributed to the anti-proliferative effect of IFN-γ in ovarian cancer cells we measured the growth of PEO1 cells in the presence of IFN-γ and the general caspase inhibitor z-VAD-FMK. The number of viable cells remaining after 96 h of exposure to IFN-γ was increased by approximately 100% in the presence of z-VAD-FMK ($P < 0.0001$) (Fig. 2(d)). This treatment also inhibited

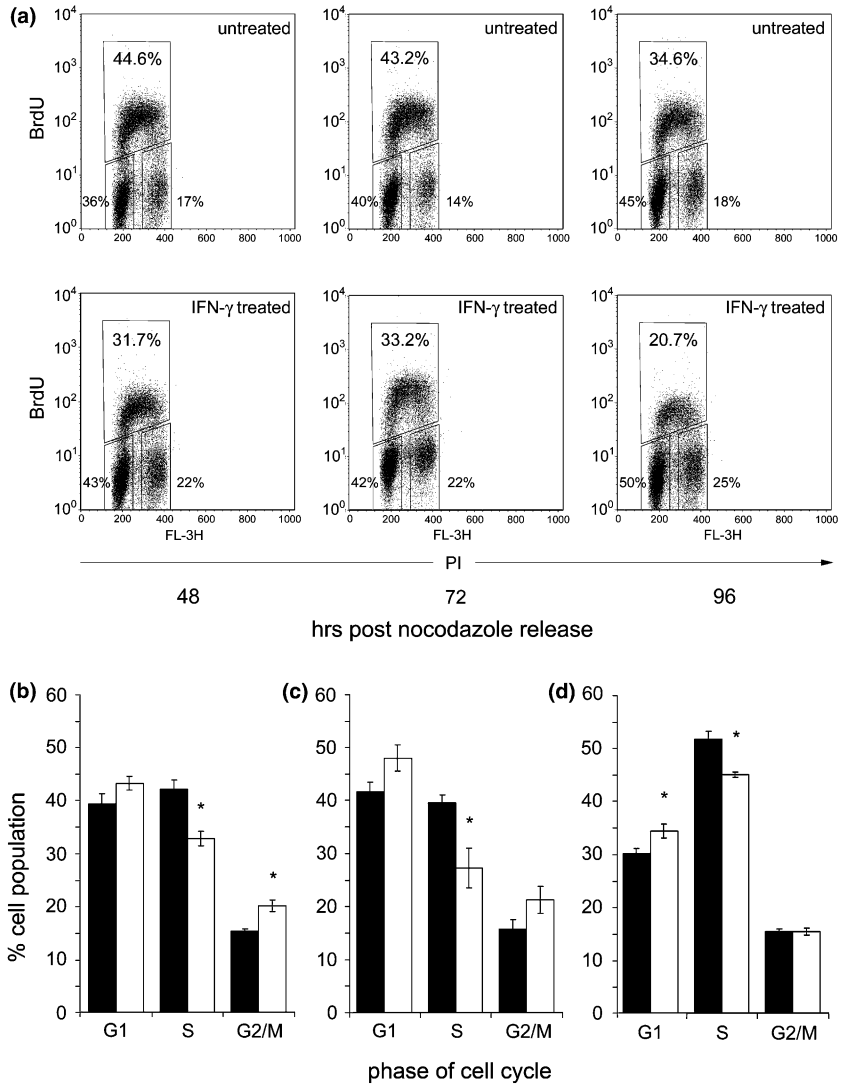

Fig. 1. BrdU analysis of synchronised ovarian cancer cells. (a) Data from a representative FACS experiment at 48–96 h after nocodazole synchronisation. Left lower region contains G1 cells, upper region contains S phase cells and right lower region contains G2 cells. The percentage of total population of PEO1 cells is shown adjacent to the marked region. (b)–(d) Graphical representation of the mean% total population of ovarian cancer cells at 72 h in each stage of the cell cycle following synchronisation: (b) nocodazole synchronised PEO1 cells; (c) hydroxyurea synchronised PEO1 cells; (d) hydroxyurea synchronised OVCAR-3 cells. ■, untreated; □, IFN-γ 5000 U/ml. Error bars represent mean ± SE, $n \geqslant 6$. * indicates $P = 0.002$–0.0001.

IFN-γ-induced PARP cleavage (Fig. 2(d), inset). Cells treated with IFN-γ displayed typical features of apoptosis: condensation of the nucleus, shrinkage of the cytoplasm and membrane blebbing. Treatment with z-VAD-FMK markedly suppressed these morphogenic changes (data not shown). Taken together, these data indicated that inhibition of caspase activity, and therefore caspase-mediated apoptosis, was partially responsible for the anti-proliferative effect of IFN-γ in sensitive cells. We therefore used immunoblotting to investigate whether activation of the apical caspases 8 and -9 played a role in the apoptotic effect of IFN-γ.

In untreated cells, caspase 8 was present predominantly in the form of the full length precursor (50/55 kDa), whilst the 23 kDa fragment of caspase 8 could be detected in PEO1 cells after 48 h of exposure to IFN-γ (Fig. 3(a)). FACS analysis using carboxyfluorescein labelled peptide inhibitor (FAM-LETD-FMK) confirmed that the cleaved subunits formed active caspases. After 72 h treatment with IFN-γ, there was a significant increase in the percentage of caspase 8 positive cells compared with untreated cells cultured for the same time (mean increase 1.9 ± 0.57, $P = 0.04$; $n = 4$) (Fig. 3(c)). Similar results were shown for OVCAR-3 cells (data not shown).

In untreated cells, caspase 9 was also present in precursor form at 47 kDa. The 35 kDa subunit of caspase 9 could be detected after 72 h of exposure to IFN-γ

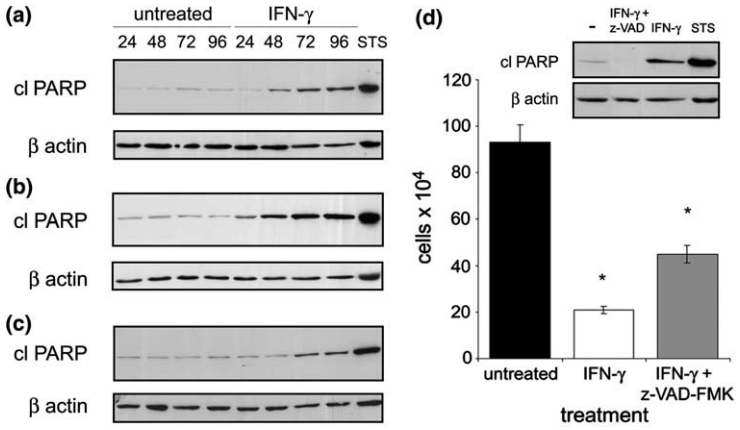

Fig. 2. IFN-γ induces PARP cleavage in a caspase-dependent manner. (a) PEO1 cells, (b) OVCAR-3 cells, (c) hydroxyurea synchronised PEO1 cells were subjected to immunoblot analysis for cleaved (cl) PARP. Cells were treated ± IFN-γ (5000 U/ml) for specified times (h). Lysates from cells treated with 1 μM STS for 6 h were used as a +ve control. (d) Immunoblot analysis of cleaved PARP after 96 h exposure to IFN-γ (5000 U/ml) and IFN-γ/z-VAD-FMK (40 μM). All blots are representative of at least two independent experiments. Also showing a graphical representation of the growth of PEO1 cells in the presence of IFN-γ and z-VAD-FMK after 96 h of exposure. ■, untreated; □, IFN-γ 5000 U/ml; ■, IFN-γ and z-VAD-FMK (40 μM). Error bars represent mean ± SE, $n = 15$. * indicates $P < 0.0001$. Incubation of PEO1 cells in the presence of z-FA-FMK, used as a control for z-VAD-FMK, or DMSO (the diluent for z-VAD-FMK) had no effect on either IFN-γ-induced PARP cleavage or growth inhibition (data not shown).

(Fig. 3(b)). Similarly, FACS analysis was performed using carboxyfluorescein labelled peptide inhibitor FAM-LEHD-FMK to confirm that the cleaved subunits formed active caspases. After 72 h treatment with IFN-γ, there was a significant mean fold increase of 2.4 ± 0.67 in the percentage of PEO1 cells that were positive for active caspase 9 when compared with untreated cells cultured for the same time ($P = 0.03$; $n = 4$), (Fig. 3(d)). Similar results were shown for OVCAR-3 cells (data not shown). These data indicated that both caspase 8 and caspase 9 were activated in PEO1 and OVCAR-3 cells in response to IFN-γ stimulation. We therefore went on to study key events involved in caspase activation.

3.4. IFN-γ treatment results in mitochondrial membrane depolarisation in PEO1 cells

The activation of caspase 9 suggested involvement of the mitochondrial-operated, or intrinsic, pathway in IFN-γ-induced cell death. IFN-induced change in mitochondrial membrane potential was investigated using MitoTracker Red CMXRos. Mitochondrial membrane depolarisation could be observed in PEO1 cells exposed to IFN-γ. Fig. 4(a) shows a representative experiment where 5.9% of IFN-γ treated cells had reduced mitochondrial membrane potential (Fig. 4(a); R2) at 72 h compared with 2.4% of untreated cells. There was a mean fold increase of 2.1 ± 0.54 in the percentage of cells with reduced mitochondrial membrane potential after 72 h IFN-γ treatment ($P = 0.01$; $n = 5$). Hoechst 33342 staining on flow sorted PEO1 cells confirmed that the R2 fraction was apoptotic (Fig. 4(b)). Shrunken, irregular nuclei were observed in the cells isolated from R2, but not in the R1 (live), fraction.

3.5. IFN-γ treatment increases the level of cytochrome c in the cytosol of ovarian cancer cells

Cytochrome *c* is released from the intermembranous spaces of mitochondria into the cytosol upon mitochondrial membrane permeabilisation. Immunoblot analysis of the cytosolic fraction of IFN-γ treated PEO1 cells showed a mean fold increase of 2.7 ± 0.47 in the level of cytochrome *c* at 72 h compared to control cells (Fig. 5(a)) ($P = 0.0003$; $n = 6$). This was abrogated in the presence of z-VAD-FMK (Fig. 5(b)), indicating a dependence on caspase activity. Similar findings were observed with OVCAR-3 cells (Fig. 5(c)).

3.6. IFN-γ induces Bid cleavage, indicating the involvement of the extrinsic apoptotic pathway

These data indicate that the mitochondrial pathway is activated following IFN-γ treatment. However, as the 23 kDa fragment of caspase 8 appeared before the 35 kDa fragment of caspase 9, and cytochrome *c* release into the cytosol was blocked by z-VAD-FMK, our data suggested that IFN-γ exerted its effect, at least in part, at a level upstream of the mitochondria. Bid, a pro-apoptotic member of the Bcl-2 family, has cytochrome *c* releasing ability when cleaved by caspase 8 into a truncated form, tBid [19,20]. Levels of intact Bid were reduced in IFN-γ treated in PEO1 and OVCAR-3 cells (Fig. 6(a) and (b)) and this was blocked by z-VAD-FMK (Fig. 6(c)).

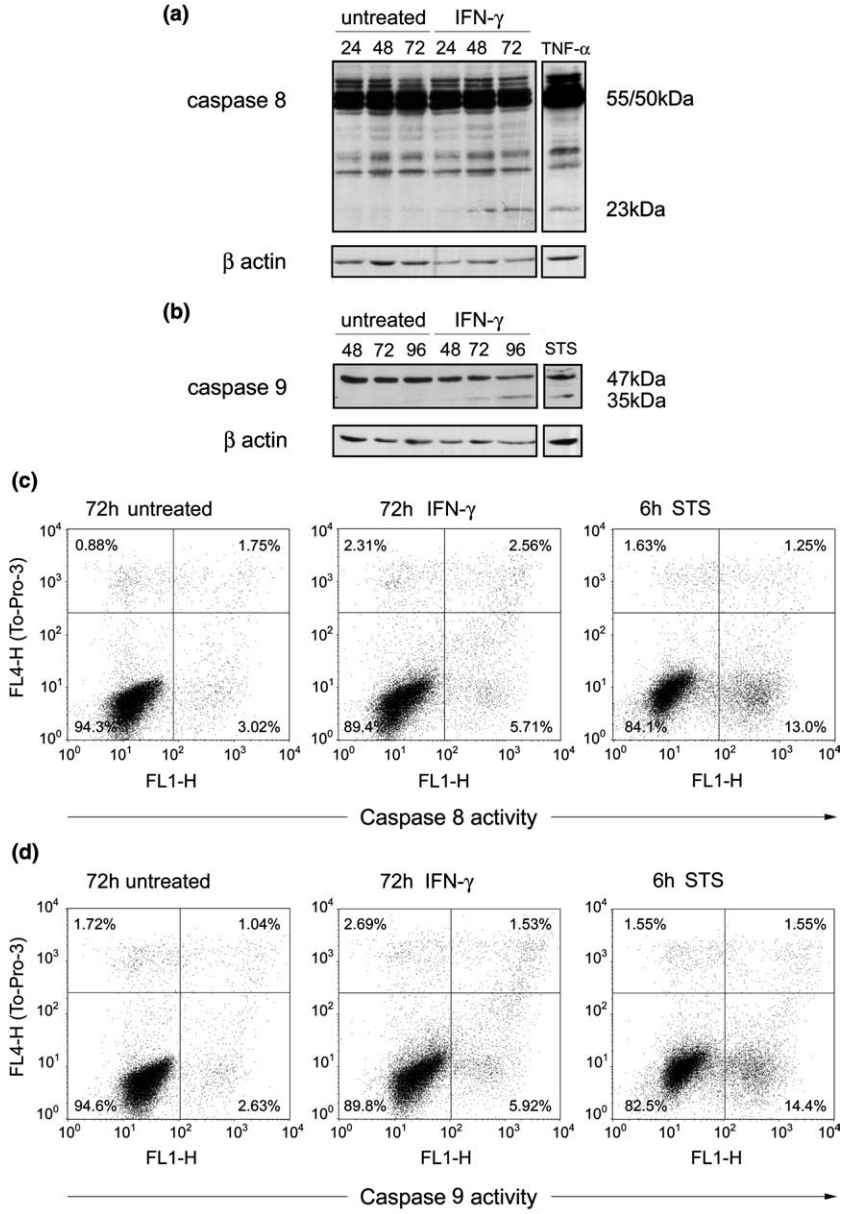

Fig. 3. Analysis of caspase 8 and caspase 9 activation in PEO1 cells. Immunoblot analysis of (a) caspase 8 and (b) caspase 9 in PEO1 cells treated ± IFN-γ (5000 U/ml) for specified times (h). Blots are representative of two independent experiments. Lysates from cells treated with 100 ng/ml TNF-α for 96 h were used as a positive control for caspase 8. Lysates from cells treated with 1 μM STS for 6 h were used as a positive control for caspase 9. FACS analysis of (c) caspase 8 activity and (d) caspase 9 activity after 72 h of treatment ± IFN-γ (5000 U/ml). Lower left quadrant contains live cells, lower right quadrant contains apoptotic cells positive for (c) FAM-LETD-FMK and (d) FAM-LEHD-FMK and upper quadrant contains dead cells. TO-PRO-3 was used as a dead cell discriminator. STS treated cells (1 μM; 6 h) were used as the positive control. Representative of four independent experiments.

3.7. Cisplatin as an anti-proliferative agent in ovarian cancer cells

As outlined in the introduction, i.p. administration of IFN-γ has anti-tumour activity in advanced stage ovarian cancer patients after clinical resistance to conventional chemotherapy has developed. We aimed to further investigate mechanisms behind the anti-proliferative effects of the combination of IFN-γ and cisplatin (the standard treatment regime). A detailed analysis of the apoptotic mechanisms behind this combination may be of use in the design of future clinical trials. In these experiments we used a lower dose of IFN-γ (200 U/ml), which we have previously demonstrated to be clinically achievable in the ascites of patients undergoing treatment for ovarian cancer with IFN-γ [5]. In

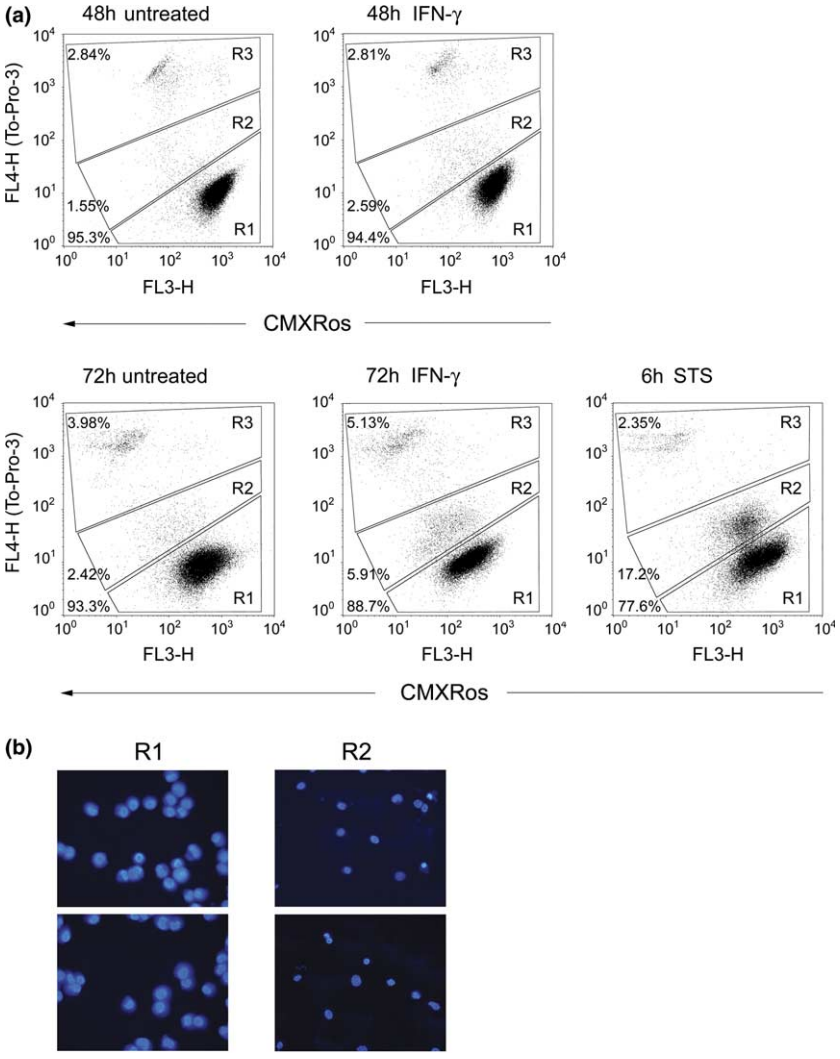

Fig. 4. Analysis of mitochondrial membrane potential in PEO1 cells. (a) FACS analysis of mitochondrial membrane potential using MitoTracker Red CMXRos ± 5000 U/ml IFN-γ treatment. Region R1 contains live cells, region R2 contains apoptotic cells and region R3 contains TO-PRO-3 +ve dead cells. The percentage of total population is shown adjacent to these regions. STS treated cells (1 μM; 6 h) were used as the positive control. Data are representative of five replicate experiments. (b) Hoechst 33342 staining on flow sorted 72 h IFN-γ (5000 U/ml) treated cells was used to confirm that R1 contained live cells and R2 contained apoptotic cells.

the same way as we did with IFN-γ alone, we first set out to assess the effects of combination treatment of both cell growth arrest and apoptosis.

Cisplatin had a time and dose-dependent anti-proliferative effect on the PEO1 cell line (Fig. 7(a)). Both 100 ng/ml and 1 μg/ml cisplatin inhibited growth of PEO1 cells after 48 h of treatment ($P = 0.0006$ and $P = 0.0325$, respectively). By 72 h the anti-proliferative effect of 1 μg/ml cisplatin was significantly greater than that of 100 ng/ml cisplatin ($P = 0.0008$). The anti-proliferative effect of 1 μg/ml and 100 ng/ml cisplatin occurred at a similar time to IFN-γ-induced growth inhibition. 100 ng/ml cisplatin was used in subsequent experiments with PEO1 cells; using a sub-optimal dose of cisplatin would allow us to distinguish any additional effects of IFN-γ.

3.8. Cisplatin increases the anti-proliferative effect of IFN-γ in PEO1 cells

As outlined in earlier studies, after 72 h of treatment with 200 U/ml IFN-γ there was a 24.5% reduction in the number of viable PEO1 cells ($P = 0.0168$). There was a 43% reduction in the number of viable PEO1 cells after cisplatin treatment ($P = 0.0001$) compared with untreated cells at the same time (Fig. 7(b)). By 96 h cisplatin reduced the number of viable cells by 71% ($P < 0.0001$) compared with untreated cells whereas, the reduction with IFN-γ was 57% ($P = 0.003$).

When cells were treated with IFN-γ and cisplatin in combination, the reduction in the number of viable cells was significantly greater compared to either IFN-γ ($P < 0.0001$) or cisplatin ($P < 0.0034$) alone after 72 h

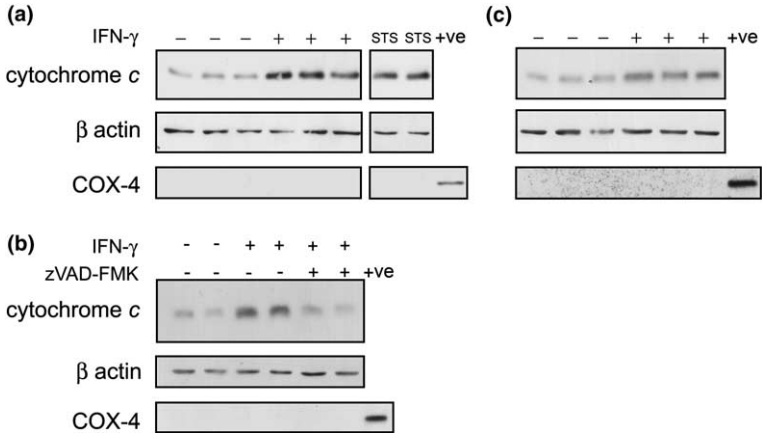

Fig. 5. Immunoblot analysis of cytosolic cytochrome *c*. Immunoblot analysis of the cytosolic fraction for cytochrome *c* after treatment ± 5000 U/ml IFN-γ. (a) PEO1 cells 72 h after treatment. STS treated cells (1 μM; 6 h) were used as the positive control for cytochrome *c* in the cytosolic fraction. (b) PEO1 cells treated ± 5000 U/ml IFN-γ or a combination of IFN-γ with 40 μM z-VAD-FMK, after 72 h. (c) OVCAR-3 cells 96 h after treatment ± IFN-γ (5000 U/ml). In each case, COX-4 was used to determine that cytosolic extracts were not contaminated with mitochondria. The mitochondrial fraction from untreated cells was used as the positive COX4 control (+ve).

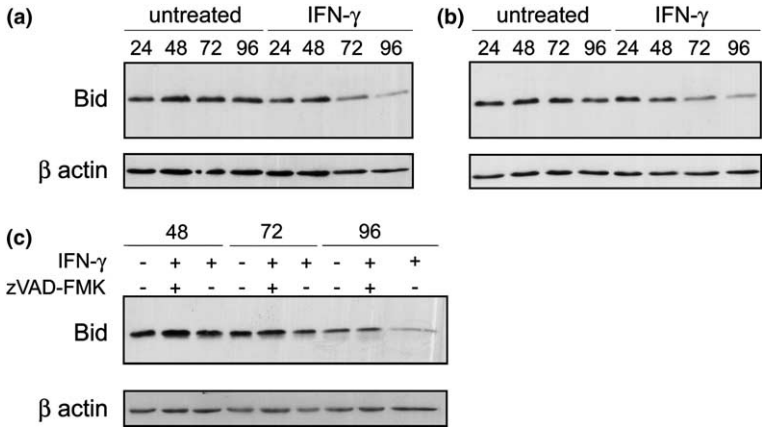

Fig. 6. Immunoblot analysis of Bid. (a) PEO1 and (b) OVCAR-3 cells at times specified (h) ± IFN-γ (5000 U/ml) treatment. (c) Bid cleavage is blocked by z-VAD-FMK (40 μM) at 72 and 96 h in PEO1 cells. Results are representative of at least three independent experiments.

and 96 h of treatment. There was a 59% reduction in cell number at 72 h ($P < 0.0001$) and 82% reduction at 96 h ($P < 0.0001$) in the number of viable PEO1 cells treated with IFN-γ and cisplatin compared with untreated cells (Fig. 7(b)).

3.9. IFN-γ-induced cell cycle blockade is augmented by cisplatin in PEO1 cells

To assess the effect of IFN-γ and cisplatin on cell cycle progression, PEO1 cells were again treated with hydroxyurea to synchronise them at the G_1–S boundary or with nocodazole to synchronize them at the G_2–M boundary. At this time cells were treated with either control media, or media containing 200 U/ml IFN-γ, 100 ng/ml cisplatin or both IFN-γ and cisplatin.

The percentage of cells synthesising DNA was significantly decreased in IFN-γ (200 U/ml) treated hydroxyurea synchronised populations compared with untreated populations 48–96 h after release ($P \leqslant 0.0073$) (Fig. 7(c) shows 72 timepoint). There was also a significant reduction in the percentage of cells synthesising DNA following treatment with cisplatin compared with untreated cells 48–96 h after release ($P \leqslant 0.0112$) (Fig. 7(c)). When cells were treated with both IFN-γ and cisplatin there was a significant further reduction compared with untreated cells at all time points. For example, the percentage of cells in S phase was reduced from 39.0% in the untreated population to 20.9% after combination treatment after 72 h treatment ($P < 0.0001$) (Fig. 7(c)). Combination treatment differed significantly from IFN-γ treatment alone at all time points ($P < 0.002$), but only significantly different to cisplatin alone at times after 72 h (Fig. 7(c)) ($P \leqslant 0.0027$).

A similar pattern was seen in the percentage of S phase IFN-γ treated cells synchronised with nocodazole.

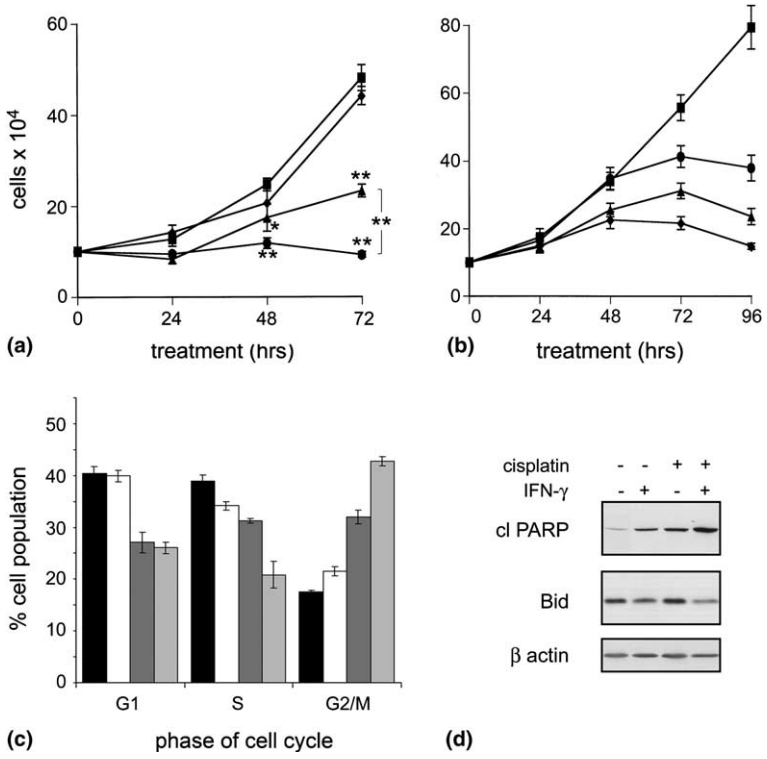

Fig. 7. Cell proliferation and death in PEO1 cells in the presence of cisplatin ± IFN-γ. (a) Cisplatin dose response curve of PEO1 cells. ■, untreated; ◆, 10 ng/ml cisplatin; ▲, 100 ng/ml cisplatin; ●, 1 μg/ml cisplatin. Error bars represent mean ± SE, $n = 3$. * indicates $P = 0.033$; ** indicates $P < 0.0008$. (b) Cell growth in the presence of cisplatin ± IFN-γ (5000 U/ml). ■, untreated; ●, 200 U/ml IFN-γ; ▲, 100 ng/ml cisplatin, ◆, 200 U/ml IFN-γ and 100 ng/ml cisplatin. Error bars represent mean ± SE, $n = 9$. Relevant P values are detailed in the text. The diluent for cisplatin was DMSO. DMSO (0.04 μl/ml) had no effect on the growth of PEO1 cells. ●● BrdU analysis of cells synchronised with hydroxyurea at 72 h. Graphical representation of the mean percentage total population in each stage of the cell cycle. ■, untreated; □, 200 U/ml IFN-γ; ■, 100 ng/ml cisplatin; ■, 100 ng/ml cisplatin and 200 U/ml IFN-γ. Error bars represent mean ± SE, $n \geqslant 6$. Relevant P values are detailed in the text. (d) Immunoblot analysis for cleaved PARP and Bid following treatment with either 200 U/ml IFN-γ, 100 ng/ml cisplatin or both (72 h). Results are representative of three independent experiments.

For example, after 72 h of combination treatment, 24.2% of cells were in S phase compared to 45.5% in the untreated population. The percentage of cells synthesising DNA following IFN-γ treatment was significantly different to untreated cells (38.8%; $P = 0.02$), as it was in cisplatin treated cells (34.5%; $P = 0.002$). Combination treatment was significantly better than either treatment alone ($P \leqslant 0.0009$). Thus, cisplatin induced a G_2-M block at all time points tested and this was augmented in the presence of IFN-γ after 72 h ($P \leqslant 0.0028$).

3.10. IFN-γ-induced PARP cleavage is augmented by cisplatin in PEO1 cells

We next looked at key molecules involved in apoptosis. In each case we used time points after 72 h as combination treatment did not differ significantly from sub-optimal cisplatin until this time. Cleaved PARP levels were increased 8-fold in PEO1 cells treated with both IFN-γ and cisplatin after 72 h of exposure when compared to untreated cells (Fig. 7(d)). This was greater than the amount of cleaved PARP detected in cells treated with one drug alone (2.4-fold increase with IFN-γ and 3.7-fold increase with cisplatin compared to untreated control).

3.11. IFN-γ-induced Bid cleavage in PEO1 cells is enhanced by cisplatin

Levels of intact Bid were decreased by two fold in PEO1 cells treated for 72 h with IFN-γ (200 U/ml) and cisplatin (100 ng/ml) (Fig. 7(d)). The decrease was greater than in cells treated with IFN-γ (200 U/ml) alone. Cisplatin treatment alone did not affect the level of intact Bid.

3.12. The mitochondrial apoptotic pathway is activated by IFN-γ and cisplatin in PEO1 cells

We investigated the intrinsic pathway in response to the combination of IFN-γ and cisplatin. Mitochondrial membrane potential was analysed using MitoTracker Red CMXRos (Fig. 8(a) shows a representative experiment). The percentage of cells with reduced mitochondrial membrane potential was increased by treatment with IFN-γ or cisplatin after 96 h (2.7% and 3.2%

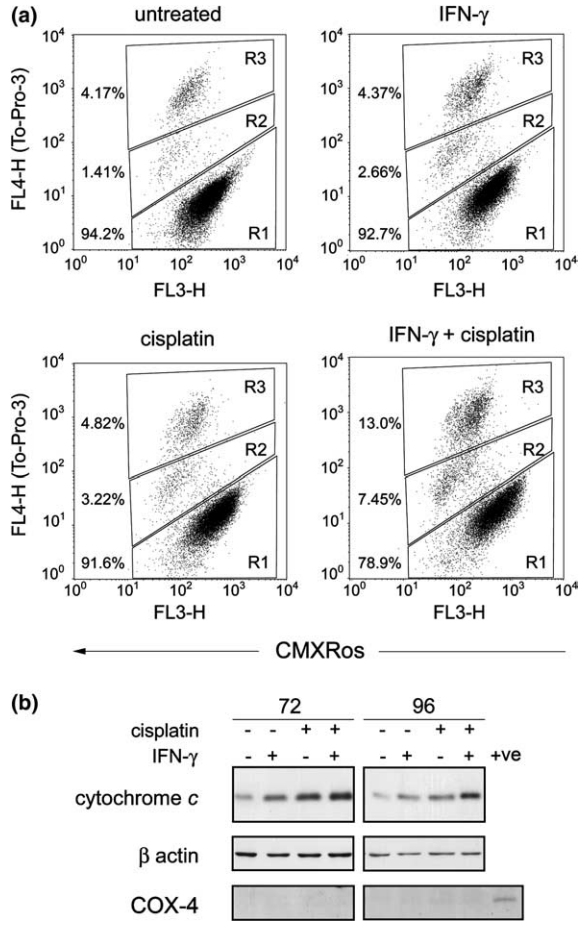

Fig. 8. Analysis of mitochondrial membrane potential and cytosolic cytochrome *c*. PEO1 cells were treated with 200 U/ml IFN-γ, 100 ng/ml cisplatin, or a combination of IFN-γ and cisplatin. (a) FACS analysis of mitochondrial membrane potential using MitoTracker Red CMXRos 96 h after treatment. Region R1 contains live cells, region R2 contains apoptotic cells and region R3 dead cells. The percentage of total population is shown adjacent to these regions. Representative of four independent experiments. (b) Immunoblot analysis of the cytosolic fraction for cytochrome *c* after 72–96 h treatment. Results are representative of two independent experiments. In each case, COX-4 was used to determine that cytosolic extracts were not contaminated with mitochondria. The mitochondrial fraction from untreated cells was used as the positive control (+ve) for COX-4.

respectively, compared with 1.4% of untreated cells). The combination of IFN-γ and cisplatin raised the amount of cells with reduced mitochondrial potential to 7.5%. This was significantly increased compared to both IFN-γ and cisplatin alone ($P < 0.0001$; $n = 4$). The amount of dead cells was also significantly increased by the combination of IFN-γ and cisplatin compared to either agent alone ($P < 0.0001$).

3.13. Cisplatin augments IFN-γ-induced release of cytochrome c into the cytosol

Immunoblot analysis of the cytosolic fraction revealed that cytochrome *c* levels in the cytoplasm were elevated in cells treated with either IFN-γ or cisplatin after 72 h and 96 h of exposure (Fig. 8(b)). At 72 h IFN-γ increased cytochrome *c* levels 2.7-fold, cisplatin increased levels of cytochrome *c* 3-fold and combination treatment increased cytochrome *c* levels 4-fold. At 96 h IFN-γ and cisplatin treatment alone increased cytochrome *c* release (2.3- and 2.5-fold compared with untreated cells respectively) and this was increased to 3.7-fold in cells treated with a combination of IFN-γ and cisplatin.

4. Discussion

We, and others, have previously determined that apoptosis (as measured, for example, by TUNEL and EM) is induced by IFN-γ in ovarian cancer cells [4,21]. In this study we have concentrated on elucidating the mechanisms by which this apoptosis occurs and subsequently looked at the contribution apoptosis makes to the well documented anti-proliferative effect of IFN-γ.

We have shown that the intrinsic apoptosis pathway was activated in response to IFN-γ in ovarian cancer cell lines. Published data on the importance of the regulation of Bcl-2 family proteins suggest a role for mitochondrial regulation of cell death in IFN-γ-treated cancer cells. For example, in gastric cancer, IFN-γ treatment resulted in increased Bak and decreased Bcl-2 expression [22]. Here we provide direct evidence for activation of this pathway by; an IFN-γ-induced collapse of mitochondrial membrane potential, cytochrome *c* release into the cytosol and caspase 9 activation. Future studies could use systems in which mitochondrial activation is blocked, for example in cell lines engineered to express Bcl-2. This would provide further evidence for a dominant role for the intrinsic pathway. Although the percentage of apoptotic cells measured after treatment were not as substantial as those observed in model systems, it is worth remembering that apoptosis in response to IFN-γ is asynchronous and the effects occur over a period of days. Our data relates to cells analysed at a snapshot in time. Thus, when z-VAD-FMK was used to inhibit apoptosis over a prolonged period, the anti-proliferative effect of IFN-γ was substantially reduced by one third.

An alternative way of activating the caspase cascade is via the death receptors and caspase 8. There is a body of evidence that suggests IFN-γ induces the expression of several members of the TNF receptor superfamily in numerous cancer cell types and thus regulates control of the extrinsic apoptotic pathway [23]. For example, CD95 is upregulated in breast cancer cells [9,10]. In this paper we have demonstrated that caspase 8 was cleaved in IFN-γ treated cells at an earlier time point than caspase 9. Moreover, when caspase activity was inhibited, cytochrome *c* release was blocked. This suggests that

caspase 8 activity upstream of the mitochondria is necessary for the activation of the mitochondrial pathway by IFN-γ in these cells.

Bid, a Bcl-2 family member normally found in the cytosol, can act to link the extrinsic and intrinsic apoptosis pathways. In the present work, levels of intact Bid decreased in IFN-γ sensitive ovarian cancer cells following IFN-γ treatment, in a caspase-dependent manner. Upon digestion by proteases, in particular caspase 8, tBid translocates to the mitochondria where it induces mitochondrial changes and strengthens the apoptotic signal. This allows for mitochondrial amplification of a weak caspase 8 signal following death receptor ligation [24]. In our system, therefore, tBid is a likely candidate in the initiation of the mitochondrial pathway in response to IFN-γ. This would certainly correlate with other data in the literature that Bid cleavage in response to certain chemotherapy agents activates the mitochondrial pathway and amplifies the apoptotic signal [25]. In summary, we conclude that the intrinsic apoptosis pathway is acting downstream of caspase 8 activation as an amplification loop following IFN-γ treatment. To confirm the importance of death receptor-mediated pathways in IFN-γ-induced apoptosis, it would be interesting in future studies to generate dominant negative FADD clones.

The anti-proliferative mechanisms by which IFN-γ exerts its effects appears to be cell type specific [26] for example, in pancreatic cancer cells IFN-γ induces apoptosis [27] and in prostate cancer cells IFN-γ induces cell growth arrest [28]. However there is little evidence from the literature investigating both responses in the same cells at the same time. By using a general caspase inhibitor we have demonstrated that both caspase-dependent apoptosis and growth arrest are important in the anti-proliferative effects of IFN-γ in ovarian cancer cells. Controversy exists in the literature over the specificity of z-VAD-FMK. Some studies suggest it can inhibit proteases other than the caspases, for example cathepsin B and -H, which can also be involved in the induction of apoptosis [29,30]. However, in the present study, when the specific cathepsin B inhibitor z-FA-FMK was added to our cells no effect on either growth inhibition or induction of apoptosis in response to IFN-γ was detected (data not shown). It is of note that the timing of the growth arrest observed in this study correlates with the induction of molecules, such as $p21^{Cip\ 1}$, responsible for blocking cell cycle progression in these cells in response to IFN-γ [4].

Whilst agents such as IFN-γ which cause cell cycle arrest and apoptosis may benefit a minority of patients, it cannot compete with the current treatment regimes such as platinum based drugs. Therefore we sought to determine whether IFN-γ could enhance the *in vitro* anti-proliferative effects of cisplatin. Earlier *in vitro* studies with IFN-γ and cisplatin in human ovarian cancer reported synergistic actions [31,32]. However, the mechanisms remain unclear since neither an increase in platinum accumulation in cells nor formation of total platinum-DNA adducts or DNA repair were thought to be responsible. A further understanding of how these two agents act together may be of benefit in the planning of future clinical studies.

Controversy exists in the literature over how chemotherapy agents such as cisplatin exert their apoptotic effects, and whether caspase 8 or -9 is the dominant apical caspase [33,34]. In this study, we showed that the intrinsic apoptosis pathway was activated in ovarian cancer cells by cisplatin, and that this was augmented by the presence of IFN-γ. In addition, cisplatin enhanced the IFN-γ-mediated reduction in the level of intact Bid. Mediators such as calpain have been associated with cisplatin cytoxicity in melanoma cells, via Bid cleavage [35] but in our cells, levels of intact Bid were not reduced by cisplatin treatment alone, either at 100 ng/ml or 1 μg/ml (data not shown). Cisplatin enhancement of the IFN-γ effect on the decrease in Bid levels, may be the result of cleavage by downstream executioner caspases as part of a positive feedback loop to act on the mitochondria, or cisplatin-mediated enhancement of extrinsic apoptosis. From these data we would hypothesise that cisplatin and IFN-γ act initially to trigger different but converging apoptotic pathways. Consequently, cellular response to death signals is maximised.

In summary, we have shown that IFN-γ mediates apoptosis in a caspase-dependent manner with both extrinsic and intrinsic pathways playing a role. Since it is clear that IFN-γ may provide therapeutic benefit to ovarian cancer patients [15], part of which may be attributed to the apoptosis of tumour cells in the ascites [5], an enhanced understanding of the molecular events underlying IFN-γ-induced apoptosis may help determine which patients are suitable for this therapy. Novel combination therapies using biological agents such as IFN-γ with chemotherapy drugs are likely to be of benefit to ovarian cancer patients. Our data provide evidence that this is a result of the targeting of both apoptotic pathways together with an enhanced G2-M arrest. Combination treatment may therefore provide a viable treatment option for ovarian cancer, especially for patients who cannot tolerate optimal doses cisplatin.

Conflict of interests statement

None declared.

Acknowledgement

This work was supported by Cancer Research UK.

References

1. Dunn GP, Old LJ, Schreiber RD. The three Es of cancer immunoediting. *Annu Rev Immunol* 2004, **22**, 329–360.
2. Malik ST, Knowles RG, East N, *et al*. Antitumor activity of gamma-interferon in ascitic and solid tumor models of human ovarian cancer. *Cancer Res* 1991, **51**(24), 6643–6649.
3. Burke F, East N, Upton C, *et al*. Interferon gamma induces cell cycle arrest and apoptosis in a model of ovarian cancer: enhancement of effect by batimastat. *Eur J Cancer* 1997, **33**(7), 1114–1121.
4. Burke F, Smith PD, Crompton MR, *et al*. Cytotoxic response of ovarian cancer cell lines to IFN-gamma is associated with sustained induction of IRF-1 and p21 mRNA. *Brit J Cancer* 1999, **80**(8), 1236–1244.
5. Wall L, Burke F, Barton C, *et al*. IFN-gamma induces apoptosis in ovarian cancer cells *in vivo* and *in vitro*. *Clin Cancer Res* 2003, **9**(7), 2487–2496.
6. Dai C, Krantz SB. Interferon gamma induces upregulation and activation of caspases 1, 3, and 8 to produce apoptosis in human erythroid progenitor cells. *Blood* 1999, **93**(10), 3309–3316.
7. Adachi Y, Taketani S, Oyaizu H, *et al*. Apoptosis of colorectal adenocarcinoma induced by 5-FU and/or IFN-gamma through caspase 3 and caspase 8. *Int J Oncol* 1999, **15**(6), 1191–1196.
8. Langaas V, Shahzidi S, Johnsen JI, *et al*. Interferon-gamma modulates TRAIL-mediated apoptosis in human colon carcinoma cells. *Anticancer Res* 2001, **21**(6A), 3733–3738.
9. Ruiz-Ruiz C, Munoz-Pinedo C, Lopez-Rivas A. Interferon-gamma treatment elevates caspase-8 expression and sensitizes human breast tumor cells to a death receptor-induced mitochondria-operated apoptotic program. *Cancer Res* 2000, **60**(20), 5673–5680.
10. Keane MM, Ettenberg SA, Lowrey GA, *et al*. Fas expression and function in normal and malignant breast cell lines. *Cancer Res* 1996, **56**(20), 4791–4798.
11. Kim KB, Choi YH, Kim IK, *et al*. Potentiation of Fas- and TRAIL-mediated apoptosis by IFN-gamma in A549 lung epithelial cells: enhancement of caspase-8 expression through IFN-response element. *Cytokine* 2002, **20**(6), 283–288.
12. Ossina NK, Cannas A, Powers VC, *et al*. Interferon-gamma modulates a p53-independent apoptotic pathway and apoptosis-related gene expression. *J Biol Chem* 1997, **272**(26), 16351–16357.
13. Balkwill F, Taylor-Papadimitriou J. Interferon affects both G1 and S+G2 in cells stimulated from quiescence to growth. *Nature* 1978, **274**(5673), 798–800.
14. Harvat BL, Jetten AM. Gamma-interferon induces an irreversible growth arrest in mid-G1 in mammary epithelial cells which correlates with a block in hyperphosphorylation of retinoblastoma. *Cell Growth Differ* 1996, **7**(3), 289–300.
15. Pujade-Lauraine E, Guastalla J-P, Colombo N, *et al*. Intraperitoneal recombinant interferon gamma in ovarian cancer patients with residual disease at second-look laparotomy. *J Clin Oncol* 1996, **14**, 343–350.
16. Windbichler GH, Hausmaninger H, Stummvoll W, *et al*. Interferon-gamma in the first-line therapy of ovarian cancer: a randomized phase III trial. *Br J Cancer* 2000, **82**(6), 1138–1144.
17. Casiano CA, Martin SJ, Green DR, *et al*. Selective cleavage of nuclear autoantigens during CD95 (Fas/APO-1)-mediated T cell apoptosis. *J Exp Med* 1996, **184**(2), 765–770.
18. Greidinger EL, Miller DK, Yamin TT, *et al*. Sequential activation of three distinct ICE-like activities in Fas-ligated Jurkat cells. *FEBS Lett* 1996, **390**(3), 299–303.
19. Luo X, Budihardjo I, Zou H, *et al*. Bid a Bcl2 interacting protein, mediates cytochrome *c* release from mitochondria in response to activation of cell surface death receptors. *Cell* 1998, **94**(4), 481–490.
20. Li H, Zhu H, Xu CJ, *et al*. Cleavage of BID by caspase 8 mediates the mitochondrial damage in the Fas pathway of apoptosis. *Cell* 1998, **94**(4), 491–501.
21. Kim EJ, Lee JM, Namkoong SE, *et al*. Interferon regulatory factor-1 mediates interferon-gamma-induced apoptosis in ovarian carcinoma cells. *J Cell Biochem* 2002, **85**(2), 369–380.
22. Shyu RY, Su HL, Yu JC, *et al*. Direct growth suppressive activity of interferon-alpha and -gamma on human gastric cancer cells. *J Surg Oncol* 2000, **75**(2), 122–130.
23. Clemens MJ. Interferons and apoptosis. *J Interferon Cytokine Res* 2003, **23**(6), 277–292.
24. Scaffidi C, Fulda S, Srinivasan A, *et al*. Two CD95 (APO-1/Fas) signaling pathways. *Embo J* 1998, **17**(6), 1675–1687.
25. Fulda S, Meyer E, Friesen C, *et al*. Cell type specific involvement of death receptor and mitochondrial pathways in drug-induced apoptosis. *Oncogene* 2001, **20**(9), 1063–1075.
26. Grander D, Einhorn S. Interferon and malignant disease—how does it work and why doesn't it always? *Acta Oncol* 1998, **37**(4), 331–338.
27. Detjen KM, Farwig K, Welzel M, *et al*. Interferon gamma inhibits growth of human pancreatic carcinoma cells via caspase-1 dependent induction of apoptosis. *Gut* 2001, **49**(2), 251–262.
28. Hobeika AC, Etienne W, Cruz PE, *et al*. IFNgamma induction of p21WAF1 in prostate cancer cells: role in cell cycle, alteration of phenotype and invasive potential. *Int J Cancer* 1998, **77**(1), 138–145.
29. Foghsgaard L, Wissing D, Mauch D, *et al*. Cathepsin B acts as a dominant execution protease in tumor cell apoptosis induced by tumor necrosis factor. *J Cell Biol* 2001, **153**(5), 999–1010.
30. Schotte P, Declercq W, Van Huffel S, *et al*. Non-specific effects of methyl ketone peptide inhibitors of caspases. *FEBS Lett* 1999, **442**(1), 117–121.
31. Nehme A, Julia AM, Jozan S, *et al*. Modulation of cisplatin cytotoxicity by human recombinant interferon-gamma in human ovarian cancer cell lines. *Eur J Cancer* 1994, **30A**(4), 520–525.
32. Nehme A, Albin N, Caliaro MJ, *et al*. Mechanism of interaction between cisplatin and human recombinant interferon gamma in human ovarian-cancer cell lines. *Int J Cancer* 1995, **61**(5), 643–648.
33. Koo MS, Kwo YG, Park JH, *et al*. Signaling and function of caspase and c-jun N-terminal kinase in cisplatin-induced apoptosis. *Mol Cells* 2002, **13**(2), 194–201.
34. Kamarajan P, Sun NK, Chao CC. Up-regulation of FLIP in cisplatin-selected HeLa cells causes cross-resistance to CD95/Fas death signalling. *Biochem J* 2003, **376**(Pt 1), 253–260.
35. Mandic A, Viktorsson K, Strandberg L, *et al*. Calpain-mediated Bid cleavage and calpain-independent Bak modulation: two separate pathways in cisplatin-induced apoptosis. *Mol Cell Biol* 2002, **22**(9), 3003–3013.